

TBA equations for excited states in the $O(3)$ and $O(4)$ nonlinear σ -model

János Balog and Árpád Hegedűs

Research Institute for Particle and Nuclear Physics,
Hungarian Academy of Sciences,
H-1525 Budapest 114, P.O.B. 49, Hungary

Abstract

TBA integral equations are proposed for 1-particle states in the sausage- and SS-models and their σ -model limits. Combined with the ground state TBA equations the exact mass gap is computed in the $O(3)$ and $O(4)$ nonlinear σ -model and the results are compared to 3-loop perturbation theory and Monte Carlo data.

1 Introduction

A better theoretical understanding of finite size (FS) effects is one of the most important problems in Quantum Field Theory (QFT). The study of FS effects is a useful method of analysing the structure of QFT models and it is an indispensable tool in the numerical simulation of lattice field theories.

Lüscher [1] derived a general formula for the FS corrections to particle masses in the large volume limit. This formula, which is generally applicable for any QFT model in any dimension, expresses the FS mass corrections in terms of an integral containing the forward scattering amplitude analytically continued to unphysical (complex) energy. It is most useful in $1 + 1$ dimensional integrable models [2], where the scattering data are available explicitly.

The usefulness of the study of the mass gap in finite volume is demonstrated [3] by the introduction of the Lüscher-Weisz-Wolff running coupling that enables the interpolation between the large volume (non-perturbative) and the small volume (perturbative) regions in both two-dimensional sigma models and QCD.

An important tool in the study of two-dimensional integrable field theories is the Thermodynamic Bethe Ansatz (TBA). This thermodynamical method was initiated by Yang and Yang [4] and allows the calculation of the free energy of the particle system. The calculation was applied to the XXZ model by Takahashi and Suzuki [5] who derived the TBA integral equations for the free energy starting from the Bethe Ansatz solution of the system and using the “string hypothesis” describing the distribution of Bethe roots.

The TBA equations also determine FS effects in relativistic (Euclidean) invariant two-dimensional field theory models where the free energy is related to the ground state energy in finite volume by a modular transformation interchanging spatial extension and (inverse) temperature. Zamolodchikov [6] initiated the study of TBA equations for two-dimensional integrable models by pointing out that TBA equations can also be derived starting from the (dressed) Bethe Ansatz equations formulated directly in terms of the (infinite volume) scattering phase shifts of the particles. In this approach the FS dependence of the ground state energy has been studied [7] in many integrable models, mainly those formulated as perturbations of minimal conformal models.

The TBA description of excited states is less complete. The excited state TBA systems first studied [8, 9] are not describing particle states, they correspond to ground states in charged sectors of the model. An interesting suggestion is to obtain excited state TBA systems by analytically continuing [9] those corresponding to the ground state energy. TBA equations for scattering states were suggested for perturbed field theory models by the analytic continuation

method [10]. Excited state TBA equations were also suggested for scattering multi-particle states for the Sine-Gordon model at its $N = 2$ supersymmetric point [11].

In [12] we proposed TBA integral equations for the excited states in the Sine-Gordon (SG) model (and massive Thirring (MT) model). Although in the SG/MT case the excited state TBA description is “superfluous” since based on the Bethe Ansatz solution of the model we already have the Destri-deVega (DdV) nonlinear integral equations [13, 14, 15] to study FS physics, the simple pattern of the excited state TBA systems we found there seems to suggest that similar systems can be found also for other models, where no DdV type alternative is available.

Our aim in this paper is to calculate the finite volume mass gap in the $O(3)$ and $O(4)$ nonlinear σ -models. These can be represented as some special limits of well-known integrable models: the sausage-model [16] and the SS-model [17] respectively. The ground state TBA equations are known for both models and although no Bethe Ansatz solution is available, based on our SG experience we make the following assumption: excited state TBA equations and Y-systems exist in these models and they are (almost) of the same form as for the ground state problem.

To transform the Y-system equations into TBA integral equations we need to know the analytic properties of the Y-system functions, in particular the distribution of their zeroes. Using Lüscher’s asymptotic formula [1] we can calculate this distribution in the infinite volume limit. Our second assumption in this paper is that the qualitative properties of this distribution remain the same for finite volume. Using this conjecture we can write down the complete set of TBA equations that are sufficient to calculate the finite volume mass gap for the sausage- and SS-models and their σ -model limits.

If both assumptions are true, the solution of the TBA problem provides the exact value of the mass gap. We have numerically computed the mass gap for both the $O(3)$ and the $O(4)$ σ -models and compared them to Monte Carlo (MC) results and 3-loop perturbation theory. The agreement with asymptotically free perturbation theory (PT) (for small volume) is especially important since our starting point was Lüscher’s formula (valid for large volume).

The paper is organized as follows. In section 2 we summarize the S-matrix data for the integrable models that are considered in this paper. In section 3 we recall the TBA integral equations and Y-systems corresponding to the ground state problem. In section 4 we briefly summarize the results of [12] for the TBA description of excited states in the SG(MT) model. In section 5 we apply Lüscher’s asymptotic formula to the integrable models of this paper and this is used in section 6 to write down the full infinite-volume solution of the Y-systems of the sausage- and SS-models and their σ -model limits. The complete TBA description of

the 1-particle states of the SS- and sausage-models are given in sections 7 and 8 respectively. Numerical solution of the TBA integral equations is discussed in section 9 and the results are compared to available MC and PT data in section 10. Finally our conclusions are summarized in section 11.

2 S-matrix data

In this section we briefly summarize the S-matrix data and some other properties of the models which will be considered in this paper.

The SG model

We first consider the Sine-Gordon model and parametrize the SG coupling as

$$\beta^2 = \frac{8\pi p}{p+1}. \quad (1)$$

For $p > 1$ we are in the repulsive regime and a soliton $|+, \theta\rangle$ and an antisoliton $|-, \theta\rangle$ of mass M form the spectrum of the model. The bootstrap S-matrix of the model is as follows [18]:

$$S_{++}^{++}(\theta) = S_{--}^{--}(\theta) = A(\theta) = -\exp\left\{i\chi\left(\frac{2\theta}{\pi}\right)\right\}, \quad (2)$$

$$\chi(\xi) = 2 \int_0^\infty \frac{dk}{k} \sin(k\xi) \tilde{g}(k), \quad \tilde{g}(k) = \frac{\sinh(p-1)k}{2 \cosh(k) \cdot \sinh(pk)}, \quad (3)$$

$$S_{+-}^{+-}(\theta) = S_{-+}^{-+}(\theta) = \kappa B(\theta), \quad (4)$$

$$B(\theta) = A(i\pi - \theta) = \frac{\sinh \frac{\theta}{p}}{\sinh \frac{i\pi - \theta}{p}} A(\theta), \quad (5)$$

$$S_{-+}^{-+}(\theta) = S_{+-}^{+-}(\theta) = C(\theta) = \frac{\sinh \frac{i\pi}{p}}{\sinh \frac{i\pi - \theta}{p}} A(\theta), \quad C(i\pi - \theta) = C(\theta). \quad (6)$$

This S-matrix is a solution of the Yang-Baxter equation, has a $U(1)$ symmetry and satisfies the usual requirements of C-, CPT- and Bose-symmetry, unitarity and real analyticity for $\kappa = \pm 1$. The sign difference between the two possible choices of κ becomes relevant in the crossing-relation:

$$S_{\alpha\beta}^{\gamma\delta}(i\pi - \theta) = C_{\beta\mu} C_{\delta\nu} S_{\alpha\nu}^{\gamma\mu}(\theta), \quad (7)$$

where $C_{\alpha\beta}$ is real and symmetric for $\kappa = +1$ and $C_{\alpha\beta}$ is imaginary and anti-symmetric for $\kappa = -1$. The physical SG model corresponds to the choice $\kappa = +1$ but we note that the above S-matrix becomes $SU(2)$ -symmetric in the limit $p \rightarrow \infty$ for the choice $\kappa = -1$.

The SS-model

The next model we consider is the SS-model [17]. There are four fundamental particles of mass M in its spectrum: $|A, \theta\rangle$, where

$$A = (\alpha_1, \alpha_2) \quad \alpha_1, \alpha_2 \in \{+, -\}. \quad (8)$$

The S-matrix of the fundamental particles [17] is:

$$\hat{S}_{AB}^{CD}(\theta) = -S_{\alpha_1\beta_1}^{\gamma_1\delta_1}(\theta) \tilde{S}_{\alpha_2\beta_2}^{\gamma_2\delta_2}(\theta), \quad (9)$$

where $S_{\alpha\beta}^{\gamma\delta}(\theta)$ is the SG S-matrix with parameter p and $\tilde{S}_{\alpha\beta}^{\gamma\delta}(\theta)$ is the SG S-matrix with parameter \tilde{p} , with the same κ parameter value. For $p, \tilde{p} > 1$ we are in the repulsive regime and there are no bound states of the fundamental particles in the model. This S-matrix satisfies the crossing relation

$$\hat{S}_{AB}^{CD}(i\pi - \theta) = \hat{C}_{BM} \hat{C}_{DN} \hat{S}_{AN}^{CM}(\theta), \quad (10)$$

where \hat{C}_{AB} is a real symmetric matrix with the following non zero matrix elements:

$$\hat{C}_{(+,+)(-,-)} = \hat{C}_{(-,-)(+,+)} = \kappa, \quad \hat{C}_{(+,-)(-,+)} = \hat{C}_{(-,+)(+,-)} = 1. \quad (11)$$

The sausage-model

There are 3 fundamental particles of mass M : $|a, \theta\rangle$, $a \in \{+, -, 0\}$ in the sausage-model [16]. When the coupling constant $0 < \lambda < \frac{1}{2}$, there are no bound states in the model. The S-matrix elements of the fundamental particles [16] are:

$$S_{++}^{++}(\theta) = S_{+-}^{+-}(i\pi - \theta) = \frac{\sinh \lambda(\theta - i\pi)}{\sinh \lambda(\theta + i\pi)}, \quad (12)$$

$$S_{+0}^{0+}(\theta) = S_{+-}^{00}(i\pi - \theta) = -i \frac{\sin 2\pi\lambda}{\sinh \lambda(\theta - 2i\pi)} \cdot S_{++}^{++}(\theta), \quad (13)$$

$$S_{-+}^{+-}(\theta) = -\frac{\sin \pi\lambda \cdot \sin 2\pi\lambda}{\sinh \lambda(\theta - 2i\pi) \cdot \sinh \lambda(\theta + i\pi)}, \quad (14)$$

$$S_{+0}^{+0}(\theta) = \frac{\sinh \lambda \theta}{\sinh \lambda(\theta - 2i\pi)} \cdot S_{++}^{++}(\theta), \quad (15)$$

$$S_{00}^{00}(\theta) = S_{+0}^{+0}(\theta) + S_{-+}^{+-}(\theta). \quad (16)$$

The $O(n)$ non-linear σ -model

The $O(n)$ NLS model consists of n self-conjugate particles: $|a, \theta\rangle$ of mass M , $a \in \{1, 2, \dots, n\}$. The S-matrix of the model is [18]:

$$S_{ab}^{cd}(\theta) = \sigma_1(\theta)\delta_{ab}\delta_{cd} + \sigma_2(\theta)\delta_{ac}\delta_{bd} + \sigma_3(\theta)\delta_{ad}\delta_{bc}, \quad (17)$$

where

$$\sigma_1(\theta) = -\frac{2\pi i \theta}{i\pi - \theta} \cdot \frac{s^{(2)}(\theta)}{(n-2)\theta - 2\pi i}, \quad (18)$$

$$\sigma_2(\theta) = (n-2)\theta \cdot \frac{s^{(2)}(\theta)}{(n-2)\theta - 2\pi i}, \quad (19)$$

$$\sigma_3(\theta) = -2\pi i \cdot \frac{s^{(2)}(\theta)}{(n-2)\theta - 2\pi i} \quad (20)$$

and the 'isospin 2' phase shift $s^{(2)}$ is given by

$$s^{(2)}(\theta) = -\exp \left\{ 2i \int_0^\infty \frac{d\omega}{\omega} \sin(\omega\theta) \cdot \tilde{K}_n(\omega) \right\} \quad (21)$$

with

$$\tilde{K}_n(\omega) = \frac{e^{-\pi\omega} + e^{-2\pi\frac{\omega}{n-2}}}{1 + e^{-\pi\omega}}. \quad (22)$$

The concrete values of the 'isospin 2' phase shift for some low values of n are:

$$n = 2 \quad s^{(2)}(\theta) = -\exp \left\{ i\chi_\infty \left(\frac{2\theta}{\pi} \right) \right\}, \quad (23)$$

$$n = 4 \quad s^{(2)}(\theta) = -\exp \left\{ 2i\chi_\infty \left(\frac{2\theta}{\pi} \right) \right\}, \quad (24)$$

$$n = 3 \quad s^{(2)}(\theta) = \frac{\theta - i\pi}{\theta + i\pi}, \quad (25)$$

where $\chi_\infty(\xi)$ is the $p \rightarrow \infty$ limit of $\chi(\xi)$.

These models can also be obtained from the models discussed previously by a limiting procedure. Concretely, the $O(2)$ model can be obtained from the SG model in the limit $p \rightarrow \infty$ [19, 20], the $O(3)$ model from the sausage-model in the limit $\lambda \rightarrow 0$ [16] and finally the $O(4)$ model from the SS-model (with $\kappa = -1$) in the limit $p, \tilde{p} \rightarrow \infty$ [17]. In the rest of the paper only the $\kappa = -1$ SS-model will be considered and called SS-model.

3 Ground state TBA equations and Y-systems

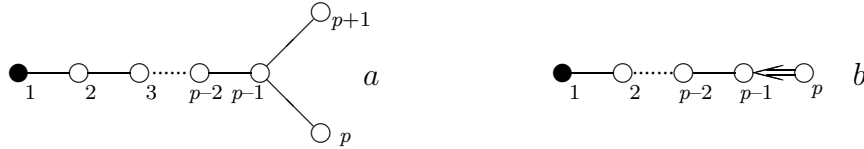


Figure 1: Dynkin-diagrams associated with D_{p+1} and A_{2p-1}^s type Y-systems.

In this section we will give a short review of the ground state TBA equations and Y-systems for the models considered in the previous section. The TBA equations of these models (at some special values of the coupling constants) can be encoded in a 'Dynkin-diagram'. The unknown functions $Y_a(\xi)$ are associated to nodes of the Dynkin-diagram and the TBA equations are of the form

$$Y_a(\xi) = e^{-l\delta_{a1} \cosh \frac{\pi}{2}\xi} e^{\beta_a(\xi)}, \quad l = ML, \quad (26)$$

where

$$l_a(u) = \sum_b I_{ab} \ln [1 + Y_b(u)], \quad (27)$$

$$\beta_a(\xi) = \frac{1}{4} \int_{-\infty}^{\infty} du \frac{l_a(u)}{\cosh \frac{\pi}{2}(u - \xi)}, \quad (28)$$

M is the mass of the particles, L is the box size and I_{ab} is the incidence matrix¹ of the Dynkin-diagram.

The ground state energy can be calculated from the solutions of the TBA equations :

$$E^{(0)} = -\frac{M}{4} \int_{-\infty}^{\infty} du \cosh \frac{\pi}{2}u \ln [1 + Y_1(u)]. \quad (29)$$

¹ I_{ab} is zero if nodes a and b are not connected by links and it is unity if the nodes are connected by a single line.

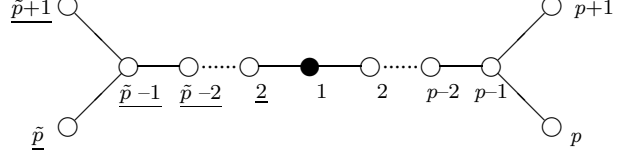


Figure 2: Dynkin-diagram associated with the SS-model Y-system (ground state).

The SG TBA equations for integer $p \geq 2$ correspond to the D_{p+1} type Dynkin-diagram shown in Figure 1a [21]. The TBA equations of the SS-model (for integer $p, \tilde{p} \geq 2$) correspond to the Dynkin-diagram shown in Figure 2 [17], finally the TBA equations of the sausage-model (for $\lambda = \frac{1}{N}$ with N integer) are associated to the Dynkin-diagram shown in Figure 3.

The solutions of these TBA equations are also solutions of the so called Y-systems [22, 23]:

$$Y_a(\xi + i)Y_a(\xi - i) = \prod_b [1 + Y_b(\xi)]^{I_{ab}}. \quad (30)$$

The standard way of solving the TBA equations is to iterate starting from the large l solution. The leading $l \rightarrow \infty$ solution of the TBA equations is easily obtained for the models discussed above. The solutions are listed below.

SG model

$$Y_1(u) \cong 2e^{-l \cosh \frac{\pi}{2} u} \quad (31)$$

$$D_p \quad \text{constant solution :} \quad \begin{cases} Y_k(u) \cong k^2 - 1 & k = 2, \dots, p-1 \\ Y_p(u) \cong Y_{p+1}(u) = p-1 \end{cases} \quad (32)$$

SS-model

$$Y_1(u) \cong 4e^{-l \cosh \frac{\pi}{2} u} \quad (33)$$

$$Y_k(u) \quad : \quad D_p \quad \text{constant solution} \quad k = 2, \dots, p+1 \quad (34)$$

$$Y_{\tilde{k}}(u) \quad : \quad D_{\tilde{p}} \quad \text{constant solution} \quad k = 2, \dots, \tilde{p}+1 \quad (35)$$

Sausage-model

$$Y_1(u) \cong 3e^{-l \cosh \frac{\pi}{2} u} \quad (36)$$

$$Y_k(u) \quad : \quad D_N \quad \text{constant solution} \quad k = 2, \dots, N+1 \quad (37)$$

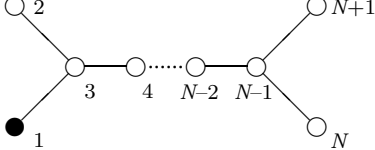


Figure 3: Dynkin-diagram associated with the sausage-model Y-system.

4 Excited states in the SG model

In this section the excited states TBA equations [12] of the SG model (and the closely related massive Thirring (MT) model) will be briefly summarized. The SG (MT) model can be regularized on a light-cone lattice in an integrable way [24]. The regularized lattice model can be solved by the Bethe Ansatz method. From the Bethe Ansatz solution of the model it follows that there exists a Y-system of the form of (30) for all excited states of the model. For simplicity in the rest of the paper we consider only the $p \geq 2$ integer case with H soliton/fermion states without antiparticles. When H is even or both H and p are odd then the corresponding Dynkin-diagram is of D_{p+1} type. In the latter case if $p \geq H$ then the D_{p+1} diagram is reduced ($Y_p = Y_{p+1} = -1$, $Y_{p-1} = 0$) to the A_{p-2} type diagram shown in Figure 4. When H is odd and p is even then I_{ab} is the incidence matrix of an A_{2p-1}^s type diagram which is shown in Figure 1b, where the oriented double line at the end of the diagram means

$$I_{p-1p} = 1, \quad I_{pp-1} = 2. \quad (38)$$

One can see that the same Y-system (30) describes a large number of different excited states of the model. The difference between the various excited state solutions of the Y-system is in the analytical structure of the solutions. The Y-system functional relations (30) can be translated into TBA integral equations in a standard way [22]. For this we have to know the positions of the zeroes and poles of $Y_a(\xi)$ in the strip $|\text{Im}\xi| < 1$ together with their asymptotic behaviour. We call this strip the main strip. From the Bethe Ansatz solution it follows that the $Y_a(\xi)$'s can have only zeroes in the main strip.

The set of zeroes of $Y_a(\xi)$ (in the main strip) will be denoted by

$$q_a = \{z_a^{(\alpha)}\}_{\alpha=1}^{Q_a}. \quad (39)$$

These zeroes are related to the T-system zeroes

$$r_a = \{y_a^{(n)}\}_{n=1}^{R_a}. \quad (40)$$

as follows.

$$q_1 = r_2, \quad q_a = r_{a-1} \cup r_{a+1} \quad a = 2, \dots, p-1 \quad (41)$$

($a = 2, \dots, p - 3$ for the A_{p-2} case) and

$$\begin{aligned} q_p = q_{p+1} &= r_{p-1} && (D_{p+1}), \\ q_p &= 2 \cdot r_{p-1} && (A_{2p-1}^s), \\ q_{p-2} &= r_{p-3} && (A_{p-2} \quad p \geq 5). \end{aligned} \tag{42}$$

With these definitions the TBA integral equations are of the form

$$Y_a(\xi) = \sigma_a e^{-l\delta_{a1} \cosh \frac{\pi}{2}\xi} \prod_{\alpha=1}^{Q_a} \tau(\xi - z_a^{(\alpha)}) \exp\{\beta_a(\xi)\}, \tag{43}$$

where σ_a is the sign of $Y_a(\infty)$ and $\tau(\xi) = \tanh\left(\frac{\pi}{4}\xi\right)$.

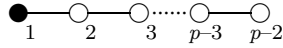


Figure 4: Dynkin-diagram associated with A_{p-2} type Y-systems.

These equations have to be supplemented by the "quantization conditions"

$$1 + Y_a(y_a^{(n)} \pm i) = 0 \quad n = 1, \dots, R_a \quad a = 1, \dots, p. \tag{44}$$

($a = 1, \dots, p - 2$ for the A_{p-2} system.) The exponential factor $e^{-l \cosh \frac{\pi}{2}\xi}$ is present in the TBA equation for $a = 1$ only. This is indicated in the figures by colouring the corresponding nodes black.

An important special case is when all zeroes are real. In this case the modulus of $Y_a(y_a^{(n)} \pm i)$ is automatically equal to unity and (44) can be rewritten as

$$(i)^{Q_a} \exp -i \left\{ \delta_{a1} l \sinh\left(\frac{\pi}{2} y_a^{(n)}\right) - \alpha_a(y_a^{(n)}) + \sum_{\alpha=1}^{Q_a} \gamma(y_a^{(n)} - z_a^{(\alpha)}) \right\} = -\sigma_a, \tag{45}$$

for $n = 1, \dots, R_a$ and $a = 1, \dots, p$ ($a = 1, \dots, p - 2$ for A_{p-2}). In (45) the notation

$$\gamma(u) = 2 \arctan(\tau(u)), \tag{46}$$

$$\alpha_a(u) = \frac{1}{4} \mathcal{P} \int_{-\infty}^{\infty} dv \frac{l_a(v)}{\sinh \frac{\pi}{2}(v - u)} \tag{47}$$

is used, where \mathcal{P} indicates principal value integration. Note that $|\gamma(u)| \leq \frac{\pi}{2}$ for real u . The quantization condition (44) for $Y_1(\xi)$

$$1 + Y_1(y_1^{(n)} \pm i) = 0 \quad n = 1, \dots, R_1 \quad (48)$$

plays a special role. The set of solutions of (48) is

$$r_1 = \left\{ y_1^{(n)} \right\}_{n=1}^{R_1}, \quad (49)$$

which includes the real zeroes $\{h_\alpha\}_{\alpha=1}^H$ (Bethe Ansatz 'holes') and complex zeroes $\{\Omega_\beta\}_{\beta=1}^C$ (complex 'holes').

The energy and momentum of the model can be easily expressed by these zeroes and by $Y_1(\xi)$:

$$E = M \left[\sum_{\alpha=1}^H \cosh \frac{\pi h_\alpha}{2} + \sum_{\beta=1}^C \cosh \frac{\pi \Omega_\beta}{2} - \frac{1}{4} \int_{-\infty}^{\infty} du \cosh \frac{\pi u}{2} \ln[1 + Y_1(u)] \right], \quad (50)$$

$$P = M \left[\sum_{\alpha=1}^H \sinh \frac{\pi h_\alpha}{2} + \sum_{\beta=1}^C \sinh \frac{\pi \Omega_\beta}{2} - \frac{1}{4} \int_{-\infty}^{\infty} du \sinh \frac{\pi u}{2} \ln[1 + Y_1(u)] \right]. \quad (51)$$

We have seen that the different states of the model are characterised by the zeroes of the Y-system and the σ_a signs. To write down TBA integral equations for a given state one needs to know the structure of zeroes of the Y-system elements and the σ_a signs for the required state. These data can be read off (at least for large enough l) from the infinite-volume solution of the Y-system. In the SG model there exists a non-linear integral equation (DdV equation) which is used to describe the Bethe Ansatz states and calculate their energy and momentum [13, 14, 15]. This equation contains only one (complex) unknown function and can easily be solved for large l in leading order (with exponential precision). The further advantage of this equation is that only those zeroes occur in it which give contribution to the energy (the set r_1). The Y-system elements can be expressed by the unknown function of the DdV equation and this way the infinite-volume solutions can be obtained from the leading order solution of the DdV equation [12]. It turns out that there are no 'complex holes' ($C = 0$) and the $l \rightarrow \infty$ solutions of the Y-system can be written in the $|\text{Im}\xi| \leq 1$ strip with exponential precision as

$$Y_1(\xi) \cong \lambda(\xi) e^{-l \cosh \frac{\pi}{2} \xi}, \quad (52)$$

$$Y_a(\xi) \cong \eta_a(\xi), \quad \begin{cases} a = 2, \dots, p-1 & D_{p+1} \\ a = 2, \dots, p & A_{2p-1}^s \\ a = 2, \dots, p-2 & A_{p-2} \end{cases} \quad (53)$$

where

$$\lambda(\xi) = (-1)^\delta \left\{ \prod_{\alpha=1}^H e^{i\chi(\xi-h_\alpha+i)} + \prod_{\alpha=1}^H e^{-i\chi(\xi-h_\alpha-i)} \right\} \quad \delta \in \{0, 1\}, \quad (54)$$

the function $\eta_2(\xi)$ is defined by

$$\lambda(\xi+i)\lambda(\xi-i) = 1 + \eta_2(\xi) \quad (55)$$

and the functions $\eta_k(\xi)$ satisfy the Y-system equations

$$\eta_k(\xi+i)\eta_k(\xi-i) = [1 + \eta_{k+1}(\xi)][1 + \eta_{k-1}(\xi)] \quad (56)$$

for $k = 2, 3, \dots$ and this determines² $\eta_k(\xi)$ for $k > 2$.

It is possible to find the solution of (56) explicitly. We note first that there is a class of solutions depending on a parameter q and a function $B(\xi)$. Using these input data we first define

$$t_0(\xi) = 0, \quad t_k(\xi) = \sum_{j=0}^{k-1} q^j B[\xi + i(k-1-2j)] \quad k = 1, 2, \dots \quad (57)$$

and then it is easy to show that

$$\eta_k(\xi) = q^{1-k} \frac{t_{k+1}(\xi)t_{k-1}(\xi)}{B(\xi+ik)B(\xi-ik)} \quad k = 1, 2, \dots \quad (58)$$

solve (56). It is also true that

$$1 + \eta_k(\xi) = q^{1-k} \frac{t_k(\xi+i)t_k(\xi-i)}{B(\xi+ik)B(\xi-ik)} \quad k = 1, 2, \dots \quad (59)$$

The actual solution entering (58) for H soliton/fermion states corresponds to the choice

$$q = (-1)^H \quad B(\xi) = \prod_{\alpha=1}^H \sinh \frac{\pi}{2p}(\xi - h_\alpha). \quad (60)$$

In the D_{p+1} case the $l \rightarrow \infty$ Y-system can be closed by defining

$$Y_p(\xi) = Y_{p+1}(\xi) = \kappa(\xi) = \frac{t_{p-1}(\xi)}{B(\xi-ip)}. \quad (61)$$

The value of the parameter δ in (54) depends on whether one is considering the Sine-Gordon model soliton states or the massive Thirring model fermion states as follows.

$$\text{SG :} \quad \delta = H \pmod{2}, \quad \text{MT :} \quad \delta = 0. \quad (62)$$

² $\eta_1(\xi) = 0$ by definition.

From this it follows that the SG and MT models are the same when H is even and different when H is odd and this difference disappears in the infinite-volume limit. In the following we summarize the infinite-volume solutions of the Y-system for the ground state and the first excited state.

$\boxed{H = 0}$ (ground state)

In this case we have a D_{p+1} system for $p \geq 2$. From (52) and (54) we get

$$\lambda(\xi) = 2(-1)^\delta. \quad (63)$$

Only the choice $\delta = 0$ is physical. Further

$$B(\xi) = 1, \quad t_k(\xi) = k, \quad \eta_k(\xi) = k^2 - 1, \quad \kappa(\xi) = p - 1. \quad (64)$$

$\boxed{H = 1}$ (one-particle state)

Here, according to (62) we have two choices:

$$\delta = 1 \quad \text{for SG}, \quad \delta = 0 \quad \text{for MT} \quad (65)$$

and we have an A_{2p-1}^s system for $p \geq 2$ even and an A_{p-2} system for $p \geq 3$ odd. The position of the hole is $h_1 = 0$ for the lowest lying excited state. This belongs to the SG case and here we restrict our attention to this case for simplicity. From (52) and (54) we find in this case

$$\lambda(\xi) = - \{ e^{i\chi(\xi+i)} + e^{-i\chi(\xi-i)} \} \quad (66)$$

and from

$$B(\xi) = \sinh \frac{\pi}{2p}(\xi) \quad (67)$$

we have

$$t_k(\xi) = \begin{cases} \frac{\cos\left(\frac{k\pi}{2p}\right)}{\cos\left(\frac{\pi}{2p}\right)} \sinh \frac{\pi\xi}{2p} & k \text{ odd} \\ i \frac{\sin\left(\frac{k\pi}{2p}\right)}{\cos\left(\frac{\pi}{2p}\right)} \cosh \frac{\pi\xi}{2p} & k \text{ even} \end{cases} \quad (68)$$

From this one can see that $Y_a(\xi)$ has no zeroes for a odd and has a double zero at $\xi = 0$ for even a values. All $Y_a(\xi)$ are negative, except $Y_p(\xi)$ in the A_{2p-1}^s case. With these analytical properties we have the following TBA equation for the first excited state.

$$Y_a(\xi) = (-1)^{1+\delta_{pa}} e^{-\delta_{a1} l \cosh \frac{\pi\xi}{2}} [\tau(\xi)]^{1+(-1)^a} \exp \{ \beta_a(\xi) \} \quad a = 1, \dots, p. \quad (69)$$

($a = 1, \dots, p-2$ for A_{p-2} .) $Y_a(\xi)$ and $\beta_a(\xi)$ are even functions and $\alpha_a(\xi)$ are odd. It follows that the quantization conditions (45) are automatically satisfied. Finally from (50) and (51) we get

$$P^{(1)} = 0, \quad E^{(1)} = M - \frac{M}{4} \int_{-\infty}^{\infty} du \cosh \frac{\pi u}{2} \ln [1 + Y_1(u)]. \quad (70)$$

5 Lüscher's formula

In this section we make the assumption that there exist TBA equations describing the finite volume dependence of the 1-particle states in the SS- and sausage-models and that these are similar to the corresponding ground state TBA equations. For large volume the solution of the TBA equations can be obtained from Lüscher's asymptotic formula, which is our starting point here.

If a stable particle in a quantum field theory is enclosed in a box, its mass changes from its infinite-volume value due to the finite-size dependence of its self-energy. Lüscher [1] derived a formula which describes the leading large-volume corrections to the mass of the lightest particle of the model in terms of the scattering amplitudes of the theory when periodic boundary conditions are imposed. This formula exists in all dimensions although it is really useful in two dimensional integrable models where the scattering amplitudes are exactly known. We discuss this formula in the simplest two dimensional case, although it exists in higher dimensions too. If there is only one mass scale in the theory and there are no bound states, the leading large-volume correction of the mass scale is

$$m(L) - M \cong -\frac{M}{2\pi} \int_{-\infty}^{\infty} d\theta \cosh \theta e^{-ML \cosh \theta} \mathcal{F}_a(\theta), \quad (71)$$

where

$$\mathcal{F}_a(\theta) = \sum_b \left[-1 + S_{ab}^{ab}(\theta + i\frac{\pi}{2}) \right] = -n + q_a(\theta + i\frac{\pi}{2}), \quad (72)$$

where n is the number of particles in the theory, $m(L)$ is the mass gap in the theory enclosed in a box of size L with periodic boundary conditions, M is the infinite-volume mass and

$$q_a(\theta) = \sum_b S_{ab}^{ab}(\theta). \quad (73)$$

When a quantum field theory is at finite temperature the virial coefficients of the pressure in the low temperature regime can be expressed by the scattering data alone [25]. The leading low temperature expression of the pressure is of the form

$$p(T) \cong \frac{T}{2\pi} nM \int_{-\infty}^{\infty} d\theta \cosh \theta e^{-\frac{M}{T} \cosh \theta}. \quad (74)$$

Using the ‘‘modular transformation’’ [2] the pressure can be related to the ground state energy of the model in a box of size L with periodic boundary conditions:

$$E^{(0)} = -L p\left(\frac{1}{L}\right) = -\frac{nM}{2\pi} \int_{-\infty}^{\infty} d\theta \cosh \theta e^{-ML \cosh \theta}. \quad (75)$$

Using the results of (75) and (71) the ground state energy ($H = 0$) and the first excited state energy ($H = 1$) of the model can be written in leading order for large L as

$$E^{(H)} = HM - \frac{M}{4} \int_{-\infty}^{\infty} du \cosh \frac{\pi}{2} u e^{-ML \cosh \frac{\pi}{2} u} y_1(u) \quad H \in \{0, 1\}, \quad (76)$$

where for the ground state energy

$$H = 0, \quad y_1(u) = n, \quad (77)$$

and for the one-particle state energy

$$H = 1, \quad y_1(u) = q_a \left(\frac{\pi}{2} (u + i) \right). \quad (78)$$

Let us assume that the TBA equations of our integrable model can be encoded in a Dynkin-diagram with one massive node and that the TBA equations of the first excited state of the model also exist. Then the energy of the ground state ($H = 0$) and the first excited state ($H = 1$) can be expressed in terms of the Y-system element associated to the massive node:

$$E^{(H)} = HM - \frac{M}{4} \int_{-\infty}^{\infty} du \cosh \frac{\pi}{2} u \ln [1 + Y_1(u)] \quad H \in \{0, 1\}, \quad (79)$$

where we assumed that the massive node of the Dynkin-diagram is indexed by one. Comparing (76) with (79) we get for $Y_1(u)$ in leading order

$$Y_1(u) \cong e^{-l \cosh \frac{\pi}{2} u} y_1(u) \quad l = ML. \quad (80)$$

Applying this formula to the ground state ($H = 0$) of the SG-, SS- and sausage-models one gets the same result for $Y_1(u)$ in leading order as that coming from the large l solution of the corresponding TBA equations, (31), (33) and (36) respectively. Thus for the ground state the leading order coefficient of the “massive” Y-system element is determined by the leading order virial coefficient.

In the previous section we have seen that (almost) the same Y-system describes all excited states of the SG model. (Small modifications occur at the end of the diagram in the odd charge sector of the model.) Calculating (78) using the scattering data (2-6) we get for the SG model

$$q(\theta) = A(\theta) + B(\theta) = -e^{i\chi(\frac{2\theta}{\pi})} - e^{i\chi(2i - \frac{2\theta}{\pi})}, \quad (81)$$

and from this we get

$$y_1(\xi) = - \left\{ e^{i\chi(\xi+i)} + e^{-i\chi(\xi-i)} \right\}. \quad (82)$$

This is the same as (66), which was obtained from the Bethe Ansatz solution of the model. This agreement makes us confident that the method works if the assumption of the existence of the first excited state TBA equations is true.

In the following we will assume that the TBA equations of the first excited state of the SS- and sausage-models also exist and they are described by almost the same Y-system as for the ground state. (The position of the massive node is the same and small modifications can occur, like in the SG model, at the end of the diagram.)

Making this assumption the leading order expression of $Y_1(u)$ can be read off (78) using the scattering data of section 2. We get for the leading order expression for $Y_1(u)$ in the SS-model

$$y_1(\xi) = -b(\xi) \tilde{b}(\xi), \quad (83)$$

where

$$b(\xi) = e^{i\chi(\xi+i)} - e^{-i\chi(\xi-i)}, \quad (84)$$

$$\tilde{b}(\xi) = e^{i\tilde{\chi}(\xi+i)} - e^{-i\tilde{\chi}(\xi-i)}. \quad (85)$$

In the sausage-model one gets different results for the charged and for the neutral particle states. The leading order result for the charged particles is

$$y_+(\xi) = y_-(\xi) = \frac{B(\xi)}{B(\xi+2i) B(\xi-2i)} \{B(\xi-2i) + B(\xi) + B(\xi+2i)\}, \quad (86)$$

where

$$B(\xi) = \sinh \frac{\lambda\pi}{2}(\xi+i) \cdot \sinh \frac{\lambda\pi}{2}(\xi-i) \quad (87)$$

and for the neutral particle states we have

$$y_0(\xi) = \frac{B(\xi)}{B(\xi+2i) B(\xi-2i)} \{3B(\xi) - \sin \pi\lambda \cdot \sin 2\pi\lambda\} \neq y_{\pm}(\xi). \quad (88)$$

Starting from these large l expressions of the “massive” Y-system elements, the $l \rightarrow \infty$ solution of the full Y-system can be obtained using the Y-system equations (30) recursively and the structure of the zeroes of the Y-system elements can be determined.

6 The $l \rightarrow \infty$ solution of the one particle Y-systems

In this section we will calculate the $l \rightarrow \infty$ solution of the Y-systems for the first excited states in the SS- and sausage-models.

The SS-model

Starting from the massive node expression (83) and applying the Y-system equations (30) recursively the infinite-volume solution of the Y-system can be obtained:

$$Y_1(\xi) \cong -e^{-l \cosh \frac{\pi}{2} \xi} b(\xi) \cdot \tilde{b}(\xi), \quad (89)$$

$$Y_k(\xi) \cong \eta_k(\xi) \quad k = 2, \dots, p, \quad (90)$$

$$Y_{\tilde{k}}(\xi) \cong \tilde{\eta}_k(\xi) \quad k = 2, \dots, \tilde{p}. \quad (91)$$

Here $\eta_k(\xi)$ is of the form (58) with $q = 1$ and

$$B(\xi) = \sinh \frac{\pi \xi}{2p}, \quad (92)$$

$$t_k(\xi) = \frac{\sin \frac{\pi k}{2p}}{\sin \frac{\pi}{2p}} \sinh \frac{\pi \xi}{2p} \quad (93)$$

and $\eta_2(\xi)$ is determined by

$$b(\xi + i) b(\xi - i) = -[1 + \eta_2(\xi)]. \quad (94)$$

Using the reflection symmetry

$$t_{p+n}(\xi) = t_{p-n}(\xi), \quad \eta_{p+n}(\xi) = \eta_{p-n}(\xi) \quad (95)$$

the diagram is closed by the relation

$$\eta_p(\xi + i) \eta_p(\xi - i) = [1 + \eta_{p-1}(\xi)]^2. \quad (96)$$

The same expressions (92-96) hold for the $\tilde{\eta}_k(\xi)$ quantities with the replacements

$$t_k(\xi) \rightarrow \tilde{t}_k(\xi), \quad \eta_k(\xi) \rightarrow \tilde{\eta}_k(\xi), \quad p \rightarrow \tilde{p}, \quad B(\xi) \rightarrow \tilde{B}(\xi).$$

This Y-system is encoded by the diagram of Figure 5. Modifications with respect to the ground state problem occur at both ends of the diagram, similarly to the SG case.

The sausage-model

Starting from the massive node expression (86) and applying the Y-system equations (30) recursively the infinite-volume solution of the Y-system of the charged particle states can be obtained:

$$Y_1(\xi) = -e^{-l \cosh \frac{\pi}{2} \xi} \eta_2(\xi), \quad (97)$$

$$Y_k(\xi) = \eta_k(\xi), \quad k = 2, \dots, N-1 \quad (98)$$

$$Y_N(\xi) = Y_{N+1}(\xi) = \kappa(\xi), \quad (99)$$

where $\eta_k(\xi)$ and $\kappa(\xi)$ can be written in the form of (58, 61) with

$$q = 1 \quad \eta_2(\xi) = y_+(\xi), \quad (100)$$

$$t_k(\xi) = \frac{\sin \lambda \pi k}{2 \sin \pi \lambda} \cosh \lambda \pi \xi - \frac{k}{2} \cos \lambda \pi, \quad (101)$$

$$\kappa(\xi) = -\frac{t_{N-1}(\xi)}{\cosh \frac{\pi}{2N}(\xi + i) \cdot \cosh \frac{\pi}{2N}(\xi - i)}. \quad (102)$$

The corresponding TBA diagram is exactly the same as for the ground state (Figure 3).

In the next two sections we will use these $l \rightarrow \infty$ solutions of the excited state Y-systems to determine the structure of zeroes of the Y-system elements, which is necessary for transforming the Y-systems into TBA integral equations. The $l \rightarrow \infty$ solutions will also be used as starting functions in the iterative numerical solution of the TBA integral equations.

7 One-particle TBA equations of the SS-model

In this section the one-particle TBA equations of the SS-model will be written down by using the analytical properties of the Y-system elements determined by the infinite-volume solution (89-96). From this we see that all $Y_a(\xi)$ functions have a double zero at $\xi = 0$ and have no other zeroes and that all $Y_a(\infty) > 0$. From these properties using (43) one can derive the following integral equation for the one-particle state.

$$Y_a(\xi) = e^{-l \delta_{a1} \cosh \frac{\pi}{2} \xi} \tau^2(\xi) e^{\beta_a(\xi)} \quad a \in \{1, 2, \dots, p, \underline{2}, \dots, \underline{p}\}. \quad (103)$$

The ‘‘quantization conditions’’ $Y_a(\pm i) = -1$ are satisfied automatically because $Y_a(\xi)$ and $\beta_a(\xi)$ are even functions and $\alpha_a(\xi)$ are odd.

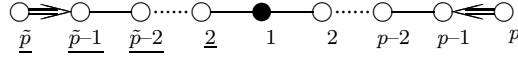


Figure 5: Dynkin-diagram associated with the SS-model Y-system (excited state).

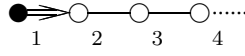


Figure 6: Dynkin-diagram associated with the $O(4)$ model Y-system.

The $O(4)$ model is the $p, \tilde{p} \rightarrow \infty$ limit of the SS-model. In this limit the Y-system consists of infinitely many components and the TBA diagram becomes symmetric to the massive node:

$$Y_k(\xi) = Y_{\underline{k}}(\xi) \quad k = 2, 3, \dots \quad (104)$$

The corresponding infinite TBA diagram is depicted in Figure 6, where the oriented double line at the beginning of the diagram means

$$I_{12} = 2, \quad I_{21} = 1. \quad (105)$$

The infinite-volume solution of the $O(4)$ model Y-system is of the form

$$Y_1(\xi) \cong -e^{-l \cosh \frac{\pi}{2} \xi} [e^{i\chi_\infty(\xi+i)} - e^{-i\chi_\infty(\xi-i)}]^2, \quad (106)$$

$$Y_k(\xi) \cong \frac{k^2 - 1}{k^2 + \xi^2} \xi^2 \quad k = 2, 3, \dots \quad (107)$$

8 One-particle TBA equations of the sausage-model

In this section the one-particle TBA equations of the sausage-model will be written down by reading off the analytical properties of the Y-system elements of the infinite-volume solution (97-102). We will consider only the generic $N \geq 5$ case. From (97-102) the signs at infinity are

$$\eta_k(\infty) > 0 \quad k = 2, 3, \dots, N-2, \quad (108)$$

$$\eta_{N-1}(\infty) < 0, \quad \kappa(\infty) < 0. \quad (109)$$

The zeroes of the infinite-volume Y-system are solutions of the equation

$$\cosh \lambda\pi H_k = \frac{k \sin 2\lambda\pi}{2 \sin k\lambda\pi}, \quad (110)$$

$$H_2 = 0; H_2 < H_3 < \dots < H_{N-1}. \quad (111)$$

All H_k 's are real and the zeroes of the infinite-volume solutions of the Y-system are

$$\eta_2 : \pm H_3, \quad (112)$$

$$\eta_3 : 0, 0; \pm H_4, \quad (113)$$

$$\eta_s : \pm H_{s-1}; \pm H_{s+1}, \quad s = 4, \dots, N-2 \quad (114)$$

$$\eta_{N-1} : \pm H_{N-2}, \quad (115)$$

$$\kappa : \pm H_{N-1}. \quad (116)$$

Using the above analytical properties one can derive the following one-particle TBA equations for the sausage-model.

$$Y_2(\xi) = \tau(\xi - H_3) \tau(\xi + H_3) e^{\beta_2(\xi)}, \quad (117)$$

$$Y_1(\xi) = e^{-l \cosh \frac{\pi}{2} \xi} Y_2(\xi), \quad (118)$$

$$Y_s(\xi) = \tau(\xi - H_{s-1}) \tau(\xi + H_{s-1}) \tau(\xi - H_{s+1}) \tau(\xi + H_{s+1}) e^{\beta_s(\xi)}, \quad s = 3, \dots, N-2, \quad (119)$$

$$Y_{N-1}(\xi) = -\tau(\xi - H_{N-2}) \tau(\xi + H_{N-2}) e^{\beta_{N-1}(\xi)}, \quad (120)$$

$$Y_N(\xi) = Y_{N+1}(\xi) = -\tau(\xi - H_{N-1}) \tau(\xi + H_{N-1}) e^{\beta_N(\xi)}. \quad (121)$$

These equations must be supplemented by the quantization conditions (44). The first two quantization conditions $Y_1(\pm i) = Y_2(\pm i) = -1$ are satisfied automatically due to the fact that $H_2 = 0$ exactly. The rest is of the form

$$\gamma(H_s - H_{s-1}) + \gamma(H_s + H_{s-1}) + \gamma(H_s - H_{s+1}) + \gamma(H_s + H_{s+1}) - \alpha_s(H_s) = 2\pi M_s, \quad (122)$$

$$s = 3, \dots, N-2$$

$$\gamma(H_{N-1} - H_{N-2}) + \gamma(H_{N-1} + H_{N-2}) - \alpha_{N-1}(H_{N-1}) = 2\pi M_{N-1}, \quad (123)$$

where

$$M_s : \text{half-integers} \quad s = 3, \dots, N - 1 \quad (124)$$

and can be determined from the infinite-volume solutions (97-102).

The $O(3)$ model is the $N \rightarrow \infty$ limit of the sausage-model, where the TBA diagram becomes infinite. In this case the infinite-volume solution becomes

$$Y_1(\xi) \cong e^{-l \cosh \frac{\pi}{2} \xi} \frac{3\xi^2 - 5}{\xi^2 + 9}, \quad (125)$$

$$Y_k(\xi) \cong \frac{(k^2 - 1) (\xi^2 - D_{k-1}) (\xi^2 - D_{k+1})}{[\xi^2 + (k - 1)^2] \cdot [\xi^2 + (k + 1)^2]}, \quad k = 2, 3, \dots \quad (126)$$

where

$$D_k = \frac{k^2 - 4}{3} \quad (127)$$

and the zeroes of the infinite-volume Y-system are of the form

$$H_k = \sqrt{D_k} \quad k = 2, 3, \dots \quad (128)$$

9 Numerical results

Our aim in this paper is to calculate the finite volume mass gap for the $O(3)$ and $O(4)$ nonlinear σ -models. Since these are the $N \rightarrow \infty$ limit of the sausage-model and the $p, \tilde{p} \rightarrow \infty$ limit of the SS-model respectively, one has to solve the TBA integral equations introduced in sections 3, 7 and 8.

Concretely, for the ground state energy ($H = 0$) we have to solve (26) of section 3. For the first excited states ($H = 1$) in the SS-model we have to solve (103) of section 7. Finally the first excited state problem in the sausage-model requires the solution of the TBA integral equations (117-121) together with the quantization conditions (122-124). After having solved the integral equations (79) can be used to calculate the energies $E^{(0)}$ and $E^{(1)}$.

For finite N (sausage-model) and finite p, \tilde{p} (SS-model) the TBA problem can easily be solved numerically by iteration. For $H = 0$ and also the $H = 1$ case of the SS-model this is completely straightforward. As usual, the $l \rightarrow \infty$ solution can be used as starting point for the iteration and the procedure converges rather rapidly. The excited state problem for the sausage-model is more involved³ since here one step in the iteration includes the calculation of the integrals occuring in (117-121) together with the calculation of the roots of (122-124).

³This is similar to the $H = 2$ problem in the SG case.

	Λ	ν	δ	ϵ	ϵ_1
$O(3)$ model $H = 0$	140	140	0.1	$10^{-6}/10^{-7}$	
$O(3)$ model $H = 1$	60	60	0.05	$10^{-5}/10^{-6}$	$10^{-7}/10^{-8}$
$O(4)$ model $H = 0$	140	140	0.1	$10^{-6}/10^{-7}$	
$O(4)$ model $H = 1$	100	60	0.1	10^{-8}	

Table 1: Parameters for numerical calculation of the ground state and first excited state energies in the $O(3)$ and $O(4)$ nonlinear σ -models. Where two values are given for ϵ and ϵ_1 the first one refers to the range $0.001 \leq l \leq 0.1$ and the second one to the range $l \geq 0.1$.

Again, the starting point of the iteration procedure is given by the $l \rightarrow \infty$ solution, both for the Y-system functions and the position of the zeroes H_s . Before the iteration is started, the half-integers in (124) have to be calculated using the large volume solution. We found that in all cases all half-integers are equal to one half.

To calculate the σ -model limit one has to take large N (or p, \tilde{p}) values and extrapolate. We adopted a slightly different approach: we studied a cutoff ∞ system. The cutoff system for the first excited states (with cutoff ν) is obtained by considering the $N = \infty$ ($p = \tilde{p} = \infty$) limit of the TBA problem but “freezing” $Y_a(\xi)$ for $a > \nu$ at the large volume limit solution, which is given by (126) and (107) for the $O(3)$ and $O(4)$ model respectively. The cutoff infinite system for the ground state problem is defined analogously. In this way we found faster convergence, probably because for the cutoff infinite system the starting point of the iteration (also for $a \leq \nu$) is the σ -model limit and thus closer to the final solution.

In Table 1 we summarized the values of the parameters we used for numerical determination of the ground state and first excited state energies for the $O(3)$ and $O(4)$ nonlinear σ -models. Here Λ is the rapidity cutoff, δ is the length of the intervals used in Simpson’s formula, ϵ is the relative precision of the numerical results for the energies and finally ϵ_1 is the accuracy of the solution of the quantization conditions (122). To the required precision (ϵ) there is no need to take better Λ , ν or δ values⁴ than those given in Table 1. With these parameter values the required precision is achieved after a few thousand iterations, which are typically completed in less than an hour on a PC. The only exception is the excited state problem for the $O(3)$ model, which requires a few hours of CPU time on a PC. Our numerical results are summarized in Tables 2 and 3. All energies are given in units of the infinite volume mass M .

⁴At least for the range $l \geq 0.001$ we consider here.

l	$\varepsilon^{(0)}$	$\varepsilon^{(1)}$
0.001	-913.954(1)	-406.23(1)
0.003	-299.5016(3)	-111.903(3)
0.01	-87.6357(1)	-23.643(1)
0.03	-28.27949(3)	-3.8325(3)
0.1	-8.006985(1)	0.77718(1)
0.3	-2.3890980(3)	1.235363(3)
1.0	-0.4862496(1)	1.084208(1)

Table 2: Numerical results for ground state and first excited state energies in the $O(3)$ nonlinear σ -model.

l	$\varepsilon^{(0)}$	$\varepsilon^{(1)}$
0.001	-1343.408(1)	-901.28159(1)
0.003	-438.1506(3)	-272.740308(3)
0.01	-127.2263(1)	-69.838028(1)
0.03	-40.60919(3)	-18.2468766(3)
0.1	-11.273364(1)	-3.0041089(1)
1/8	-8.8346989(8)	-1.91603183(8)
1/4	-4.0487295(4)	-0.00446984(4)
1/2	-1.7404694(2)	0.71072801(2)
1	-0.6437746(1)	0.93839706(1)
2	-0.16202897(1)	0.99233406(1)
4	-0.01562574(1)	0.99965327(1)

Table 3: Numerical results for ground state and first excited state energies in the $O(4)$ nonlinear σ -model.

10 Monte Carlo and perturbative results

We are now in a position to be able to compare our numerical results with those of Monte Carlo simulations and perturbative calculations. Checking our results using asymptotically free perturbation theory (PT) in the small volume ($l \rightarrow 0$) limit is especially important since our construction is based on Lüscher's formula and the large volume ($l \rightarrow \infty$) solution.

Perturbative calculations for the finite volume mass gap of the $O(n)$ nonlinear σ -model

$$z(l) = LM(L) = l [\varepsilon^{(1)}(l) - \varepsilon^{(0)}(l)] \quad (129)$$

are available up to three loop order [26]. The results are best presented in the form of the asymptotic expansion

$$z(l) = \frac{\pi(1 + \Delta)}{x} \left\{ 1 + \frac{\Delta}{x^2} + \frac{u_3}{x^3} + \dots \right\}, \quad (130)$$

where $\Delta = 1/(n - 2)$ and the (inverse) running coupling x is the solution of the equation

$$x - \Delta \ln x = \ln \left(\frac{1}{L\Lambda_{\text{FV}}} \right). \quad (131)$$

The perturbative lambda parameter used here is the Finite Volume lambda, which is best suited to the problem [26] and is related to the conventional $\Lambda_{\overline{\text{MS}}}$ by

$$\Lambda_{\text{FV}} = \frac{e^\gamma}{4\pi} \Lambda_{\overline{\text{MS}}} = \frac{e^\gamma}{4\pi} \left(\frac{e}{8} \right)^\Delta \Gamma(1 + \Delta) M. \quad (132)$$

Here γ is Euler's constant and in the second equality we have used the exact value of the $M/\Lambda_{\overline{\text{MS}}}$ ratio, which is available for this family of models [27].

The coefficient of the three-loop contribution is [26]

$$u_3 = \frac{\chi_1}{8} + \frac{\chi_2}{8} \Delta + \frac{\chi_3}{8} \Delta^2 + \left(\frac{\chi_4}{8} - \frac{1}{2} \right) \Delta^3, \quad (133)$$

where

$$\begin{aligned} \chi_1 &= -1.2020569, & \chi_3 &= 23.6, \\ \chi_2 &= -3.63, & \chi_4 &= -5.2123414. \end{aligned} \quad (134)$$

In terms of the physical volume l we have to solve

$$x - \Delta \ln x = \ln \left(\frac{1}{l} \right) - \omega_1, \quad (135)$$

where

$$\omega_1 = \gamma - \ln 4\pi + \Delta \ln \left(\frac{e}{8} \right) + \ln \Gamma(1 + \Delta). \quad (136)$$

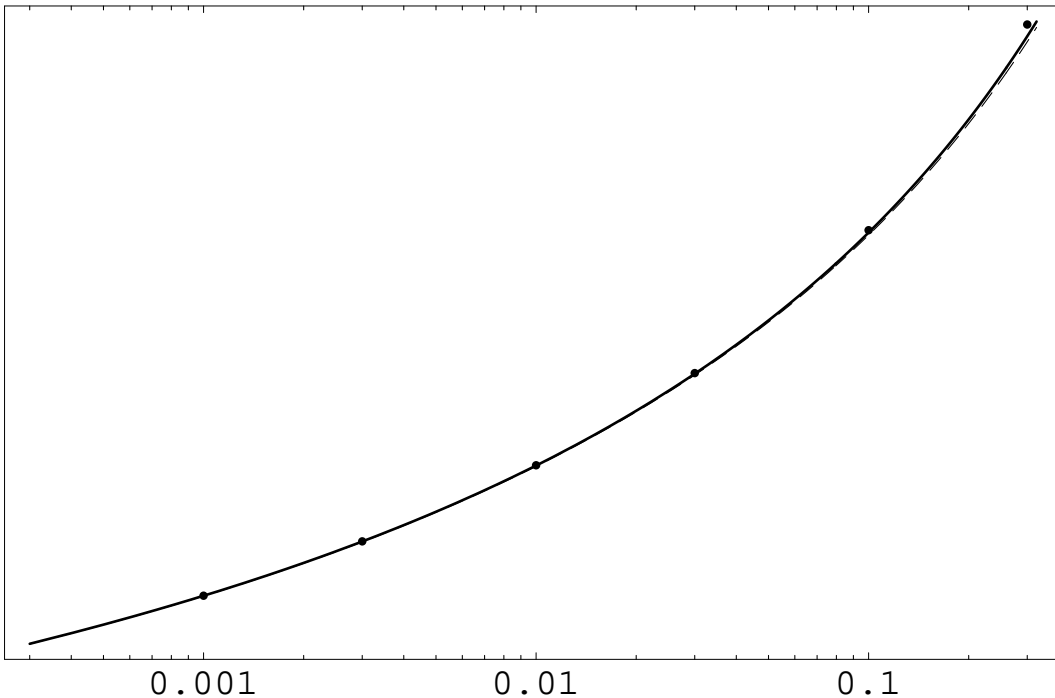


Figure 7: Finite volume mass gap of the $O(3)$ model. Comparison of numerical solution of the TBA integral equations (dots) to three-loop perturbation theory (solid line). The two-loop perturbative curve (dashed line) is also shown.

The comparison of our numerical results to the three-loop perturbative predictions is shown in Figures 7 and 8. It is reassuring to see that our results agree very well with asymptotically free PT in the small volume regime.

In Table 4 we collected all available data on the finite volume mass gap for the $O(4)$ model. In addition to our numerical results the three-loop perturbative results (for small volumes), results of MC simulations [28] and (for large volumes) the values corresponding to Lüscher’s formula are given.

Some MC results are available also for the $O(3)$ model. We intend to discuss how they compare to the results of the TBA calculations presented in this paper in a future publication. Here we only mention that we have calculated the value of the “step scaling function” [3] $\sigma(2, u_0)$ at the “canonical” point $u_0 = 1.0595$. We found

$$\sigma(2, u_0) = 1.261208(1), \tag{137}$$

which seems to support the results of the form-independent fit in [29].

l	TBA	PT	MC	Lüscher
0.001	0.442126	0.442097		
0.003	0.496231	0.496176		
0.01	0.573883	0.573766		
0.03	0.670869	0.670606		
0.1	0.8269255	0.826130		0.4733
1/8	0.8648334	0.863821	0.863(2)	0.5265
1/4	1.0110649	1.00868	1.011(2)	0.7368
1/2	1.2255987	1.21867	1.228(2)	1.0395
1	1.5821717		1.584(4)	1.4941
2	2.3087261		2.309(10)	2.2909
4	4.0611160		4.132(10)	4.0607

Table 4: Results for the finite volume mass gap $z(l)$ in the $O(4)$ nonlinear σ -model.

11 Summary and conclusion

In this paper we proposed TBA integral equations for the 1-particle states in the sausage- and SS-models and for their σ -model limits, for the $O(3)$ and $O(4)$ nonlinear σ -models respectively. The excited state TBA systems are based on analogy with the corresponding problem in the Sine-Gordon model and the solution in the large volume limit, which can be obtained from Lüscher's asymptotic formula. Combining the 1-particle TBA systems with those corresponding to the ground state we can calculate the exact value of the mass gap numerically for the sausage- and SS-models, and, by extrapolation, also for their σ -model limits, which correspond to infinite TBA systems. We have proposed a somewhat different, more efficient method to treat these infinite TBA systems: instead of taking larger and larger sausage-model (or SS-model) TBA systems and extrapolating, we consider directly the infinite system, with a cutoff that removes the remote TBA nodes. Considering the cutoff infinite system instead of the original problem leads to faster convergence of the iteration procedure and produces numerically precise results for the σ -model mass gap already at moderate values of the cutoff parameter.

Having computed the mass gap for the $O(3)$ and $O(4)$ models we can compare the results to those of lattice Monte Carlo simulations and perturbation theory. We have observed perfect agreement taking account of all available data. Since the σ -models are asymptotically free, the perturbative results are reliable at small volumes. On the other hand our TBA systems are based on Lüscher's large volume asymptotic formula and hence the very good agreement of

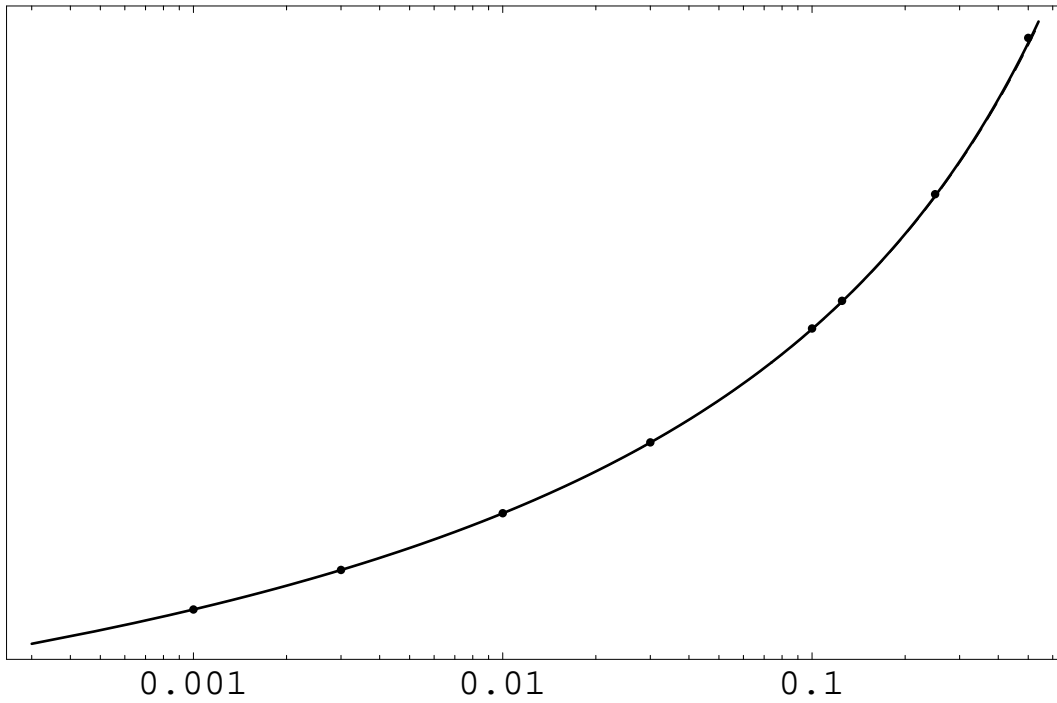


Figure 8: Finite volume mass gap of the $O(4)$ model. Comparison of numerical solution of the TBA integral equations (dots) to three-loop perturbation theory (solid line). The two-loop perturbative result is too close to the three-loop result and is not shown here.

the perturbative results with our numbers for small volumes indicate that all our assumptions leading to the excited state TBA systems are valid. The lattice Monte Carlo data are for the intermediate volume range and the results agree with our mass gap values within the Monte Carlo errors. Thus we have numerically checked the correctness of the proposed TBA equations for a large volume range between $l \sim 1$ and $l \sim 10^{-3}$.

Acknowledgements

This investigation was supported in part by the Hungarian National Science Fund OTKA (under T034299 and T043159).

References

- [1] M. Lüscher, *Comm. Math. Phys.* **104** (1986) 177; **105** (1986) 153.

- [2] T. R. Klassen and E. Melzer, Nucl. Phys. **B362** (1991) 329.
- [3] M. Lüscher, P. Weisz and U. Wolff, Nucl. Phys. **B359** (1991) 221.
- [4] C. N. Yang and C. P. Yang, J. Math. Phys. **10** (1969) 1115.
- [5] M. Takahashi and M. Suzuki, Prog. Theor. Phys. **48** (1972) 2187.
- [6] Al. B. Zamolodchikov, Nucl. Phys. **B342** (1990) 695.
- [7] T. R. Klassen and E. Melzer, Nucl. Phys. **B338** (1990) 485; **B350** (1991) 635;
Al. B. Zamolodchikov, Nucl. Phys. **B358** (1991) 497; **B366** (1991) 122;
V. A. Fateev and Al. B. Zamolodchikov, Phys. Lett. **B271** (1991) 91;
F. Ravanini, R. Tateo and A. Valleriani, Int. J. Mod. Phys. **A8** (1993) 1707;
R. Tateo, Phys. Lett. **B355** (1995) 157;
P. Fendley, Phys. Rev. Lett. **83** (1999) 4468.
- [8] P. Fendley, Nucl. Phys. **B374** (1992) 667.
- [9] M. J. Martins, Phys. Rev. Lett. **67** (1991) 419.
- [10] P. Dorey and R. Tateo, Nucl. Phys. **B482** (1996) 639; **B515** (1998) 575.
- [11] P. Fendley, Adv. Theor. Math. Phys. **1** (1998) 210.
- [12] J. Balog and Á. Hegedűs, [hep-th/0304260](#).
- [13] C. Destri and H. J. de Vega, Phys. Rev. Lett. **69** (1992) 2313; Nucl. Phys. **B438** (1995) 413.
- [14] C. Destri and H. J. de Vega, Nucl. Phys. **B504** (1997) 621;
G. Feverati, F. Ravanini and G. Takács, Phys. Lett. **B430** (1998) 264; Nucl. Phys. **B540** (1999) 543.
- [15] G. Feverati, F. Ravanini and G. Takács, Phys. Lett. **B444** (1998) 442.
- [16] V. A. Fateev, E. Onofri and Al. B. Zamolodchikov, Nucl. Phys. **B406** [FS] (1993) 521.
- [17] V. A. Fateev, Nucl. Phys. **B473** [FS] (1996) 509.
- [18] A. B. and Al. B. Zamolodchikov, Ann. Phys. **120** (1979) 253;
Nucl. Phys. **B133** (1978) 525.

- [19] J. Zinn-Justin, *Quantum Field Theory and Critical Phenomena*, Oxford, 1989.
- [20] D. J. Amit, Y. Y. Goldschmidt and G. Grinstein, *J. Phys.* **A13** (1980) 585.
- [21] M. Fowler and X. Zotos, *Phys. Rev.* **B26** (1982) 2519.
- [22] A. Kuniba, K. Sakai and J. Suzuki, *Nucl. Phys.* **B525** [FS] (1998) 597.
- [23] Al. B. Zamolodchikov, *Phys. Lett.* **B253** (1991) 391; *Nucl. Phys.* **B358** (1991) 497, 524.
- [24] C. Destri and H. J. de Vega, *Nucl. Phys.* **B290** (1987) 363; *J. Phys.* **A22** (1989) 1329.
- [25] R. Dashen, S. Ma and H. J. Bernstein, *Phys. Rev.* **187** (1969) 345.
- [26] D.-S. Shin, *Nucl. Phys.* **B496** (1997) 408; *Nucl. Phys.* **B546** (1999) 669.
- [27] P. Hasenfratz, M. Maggiore and F. Niedermayer, *Phys. Lett.* **B245** (1990) 522;
P. Hasenfratz and F. Niedermayer, *Phys. Lett.* **B245** (1990) 529.
- [28] M. Hasenbusch and R. R. Horgan, *Phys. Rev.* **D53** (1996) 5075.
- [29] M. Hasenbusch, P. Hasenfratz, F. Niedermayer, B. Seefeld and U. Wolff,
Nucl. Phys. Proc. Suppl. **106** (2002) 911.